European Review for Medical and Pharmacological Sciences 2023; 27: 11370-11382

Roxadustat protects rat renal tubular epithelial cells from hypoxia-induced injury through the TGF-β1/Smad3 signaling pathway

F.-F. ZHENG[1,2], Y.-Y. ZHAO[1,2], L.-J. CAI[1,2], G. WU[1,2], J.-N. WANG[1,2], M.-Z. ZHAO[1,2]

[1]The Affiliated Suqian Hospital of Xuzhou Medical University, Jiangsu, Suqian, China
[2]Nanjing Drum Tower Hospital Group Suqian Hospital, Jiangsu, Suqian , China

F.-F. Zheng and Y.-Y. Zhao contributed equally to this work

Abstract. – OBJECTIVE: Roxadustat is used to treat renal anemia. The renoprotective effect of roxadustat needs to be further confirmed, and the mechanism of action is unknown. This study aims to evaluate the effect and mechanism of roxadustat in hypoxia-related nephropathy with the renal tubular epithelial cell line NRK-52E.

MATERIALS AND METHODS: The cell Counting Kit-8 (CCK-8) assay was employed to assess cellular proliferation in the current investigation. Flow cytometry was used to conduct cell apoptosis analysis. The utilization of electron microscopy facilitated the identification of changes in cellular ultrastructure. Immunofluorescence was used to detect the expression trend of hypoxia-inducible factor-1α (HIF-1α). The connective tissue growth factor (CTGF), transforming growth factor-β1 (TGF-β1), Smad family member 3 (Smad3), p-Smad3, α-smooth muscle actin (α-SMA), collagen I, and HIF-1α were assessed by western blotting. Real-time fluorescent quantitative PCR (RT-qPCR) was used to measure TGF-β1 and Smad3 mRNA.

RESULTS: Significant growth inhibition and increased apoptosis were observed in NRK-52E cells cultured under hypoxic conditions (1% and 5% O_2), which can be rescued by roxadustat. From a morphological perspective, it has been observed that roxadustat can counteract cellular damage features produced by hypoxia. These features include the contraction of the nuclear envelope and an increase in the formation of apoptotic bodies. Roxadustat increases HIF-1α expression acutely at 24 h, followed by a gradual reduction of HIF-1α expression to levels significantly below that of the hypoxia group by 72 h. Roxadustat can also inhibit hypoxia-induced increased expression of CTGF, TGF-β1, p-Smad3, α-SMA, collagen I, and HIF-1α. Combined treatment with roxadustat and siRNA against TGF-β1 synergistically reduced the expression of CTGF and HIF-1α, while the effect on TGF-β1 and p-Smad3 were comparable to that of the individual treatment alone. Comparably, the combined administration of roxadustat and siRNA targeting Smad3 had a synergistic impact on diminishing the expression of CTGF.

CONCLUSIONS: These findings indicate that roxadustat attenuates experimental renal fibrosis likely by inhibiting the TGF-β1/Smad3 pathways, while its effect on CTGF and HIF-1α may involve other signaling pathways.

Key Words:
Roxadustat, Hypoxia, Renal injury, TGF-β1/Smad, NRK-52E.

Introduction

Roxadustat is a pharmacological agent that functions as an inhibitor of hypoxia-inducible factor prolyl hydroxylase. It has exhibited both safety and efficacy in treating renal anemia[1,2]. Nevertheless, renal-protective effects and their association with signaling pathways remain uncertain. Recent studies[3,4] showed that roxadustat attenuates experimental pulmonary fibrosis *in vitro* and *in vivo* and markedly reduces myocardial ischemia-reperfusion injury in mice. Nevertheless, research is scarce on the potential protective effects of kidney injury. Our previous clinical studies[5] have shown that roxadustat can reduce the expression of serum transforming growth factor-β1 (TGF-β1) and fibronectin (FN) in patients with renal anemia, suggesting that roxadustat may have a protective effect on the kidney. However, additional research is necessary to validate these data and investigate the underlying mechanism of action.

Hypoxia is an inherent pathophysiological characteristic of chronic kidney disease (CKD) and is closely associated with the development

Corresponding Author: M.-Z. Zhao, MD; e-mail: zhaomingzuo@163.com

of renal fibrosis[6]. The proximal tubule is particularly vulnerable to injuries such as hypoxia, which may be related to the high concentration of mitochondria in these cells and the dependency on oxidative phosphorylation. Tubular epithelial cells are susceptible to both inflammation and fibrogenesis. A growing body of evidence[7] indicates that when exposed to hypoxia, these cells suffer functional changes such as cell death or atrophy, maladaptive repair, metabolic switching, and senescence. Additionally, they release a range of bioactive substances that contribute to interstitial inflammation and fibrosis.

Hypoxia can cause epithelial-mesenchymal transition (EMT) in the kidney, leading to renal fibrosis[8]. EMT is characterized by a decrease of the epithelial marker E-cadherin and an increase of the mesothelial marker α-smooth muscle actin (α-SMA). Increased expression of other proteins, such as connective tissue growth factor (CTGF), collagen I, and collagen III, has also been associated with renal fibrosis[9]. Our previous studies[10,11] showed that roxadustat can reduce the expression of TGF-β1 in serum. The TGF-β1/Smad signaling pathway plays a crucial role in the pathogenesis of fibrosis. TGF-β1 is a multifunctional cytokine that participates in inflammation, cell growth, apoptosis, and differentiation in the formation of tissue fibrosis[12]. The Smad protein family is the downstream substrate molecules of TGF-β1 signaling and are categorized as receptor-activated, universal, or inhibitory types depending on their structure. The receptor-activated Smad3 can bind directly to the promoter region of collagen to promote renal fibrosis[13].

In this study, we aimed to evaluate the ability of roxadustat to protect against hypoxia-induced cell injury, focusing on signaling mechanisms involving TGF-β1, Samd3, p-Samd3, CTGF, hypoxia-inducible factor-1α (HIF-1α), α-SMA, and collagen I.

Materials and Methods

Cell Culture

NRK-52E cells (Procell, Wuhan, China) were cultured in Dulbecco's Modified Eagle Medium (DMEM) supplemented with 10% fetal bovine serum and maintained at 37°C and 5% CO_2. Cells were grown until confluent, then used in experiments. All media and supplements were purchased from GENOM (Guangzhou, China).

Hypoxia and Roxadustat Treatment

Experimental hypoxia can be generated chemically with a HIF-1 inducer (cobalt chloride, $CoCl_2$)[14] or with a three-system incubator by controlling the input of O_2, N_2, and CO_2. Three-gas incubator-generated hypoxia models have been used to study kidney injury[15,16]. We adopted a similar system to culture cells under hypoxic (1, 5, or 10% O_2) conditions using a three-system incubator (Heal Force, Shanghai, China). Roxadustat (S1007, Selleck, Houston, USA) was dissolved in the Division Medical Supply Office (DMSO) and prepared as a stock solution (20 mM) with Phosphate Buffer Saline (PBS). The stock solutions were diluted in serum-free medium to give a final concentration of 0.3, 1, 3, 10, and 15 mM for experiments.

Cell Proliferation Assay

NRK-52E cells were seeded into 96-well plates at a density of $1x10^3$ cells/well and incubated in normal oxygen concentration (21% O_2) for 24 h, followed by a medium change and incubation at different O_2 concentrations (1%, 5%, 10%, 21%) for 24, 48 and 72 h. The cell Counting Kit-8 (CCK-8) solution (10 μL) was added to each well and incubated for 4 h, and the absorbance was measured at 450 nm on a Diatek microplate reader (R-200Bs, Jiangsu, China).

Apoptosis Measurement by Flow Cytometry

Cells were seeded into 6-well plates and cultured for 72 h, then, washed with PBS and collected into flow tubes. Cells precipitate were resuspended with 300 μL binding buffer, then, permeabilized with 0.25% trypsin, stained with annexin V-FITC, and the mixture was incubated in the dark for 10 min. After adding 5 μL PI, the mixture was incubated in the dark for 5 min and analyzed using flow cytometry (CytoFlex, Beckman, Germany) within 1 hour.

HIF-1α Measurement by Immunofluorescence

Cells were cultured for 24, 48, and 72 h and fixed with 4% formaldehyde, stained with primary antibody against HIF-1α (1:100, Abcam, Cambs, UK) overnight, and anti-rabbit-CY3 secondary antibody (1:100, Aspen, Wuhan, China). Nuclei were stained with the Diamidino Phenylindole (DAPI). Stained cells were viewed and imaged with a fluorescence microscope

(IX51, Olympus, Japan). The Ipwin32 software (Bethesda, MD, USA) was used to quantify fluorescence intensity.

Electron Microscopy

Cells were cultured for 72 h, washed, and processed for transmission electron microscopy (TEM), including fixation, dehydration, embedding, slicing, and uranyl acetate dye staining. First, the cells were rinsed 15 min with pH 7.2 phosphate buffer three times and then fixed with 1% hungry acid for 2 h, using ethanol concentration gradients of 45%, 55%, 70%, 85%, 95%, 100% I, and 100% II to dehydrate. Epon812 resin was used in infiltration, embedding and polymerization. Trimming and sectioning were performed with a 60-70 nm ultra-thin microtome. Then stained with 100 uL of 50% ethanol saturated solution of uranyl acetate for 15-100 min, rinsed with double distilled water, and stained with 100 uL of lead citrate for 15 min. Cells were observed on the FEI (TECNAI G2 SPIRIT, MA, USA).

Western Blotting

Cells were cultured for 72 h and washed with ice-cold PBS. Proteins were extracted with the whole-cell extraction kit (Keygen Biotech, Beijing, China) and quantified using the BCA method (Keygen Biotech, Beijing, China). 40 μg of proteins were separated by Sodium Dodecyl Sulfate-Polyacrylamide Gel Electrophoresis (SDS-PAGE) and transferred to nitrocellulose membranes. Membranes were incubated overnight at 4°C with primary antibodies against TGF-β1 (1:2000, Wuhan Sanying biotech, Wuhanm, China), CTGF (1:3000, Wuhan Sanying biotech, Wuhan, China), Smad3 (1:3000, CSH, MA, USA), p-Smad3 (1:500, CSH, MA, USA), HIF-1α (1:1000, CSH, MA, USA), α-SMA (1:100, Abcam, Cambs, UK), collagen I (1:1000, Abcam, Cambs, UK) and β-Actin (1:10000, Beijing TGY Biotech, Beijing, China). Detection was performed with secondary Goat Anti-Rabbit Horseradish Peroxidase (HRP) (1:10000, Aspen, Wuhan, China) and Electro Chemiluminescence (ECL) reagent (Aspen, Wuhan, China). Immunoreactive bands were quantified using an Imaging System (Bio-RAD, Berkeley, CA, USA). Values were corrected with the internal control (β-actin).

siRNA and RT-QPCR

siRNAs against TGF-β1 and Smad3 were synthesized using Ribobio (Guangzhou, China) according to the sequences in Table I.

For RT-QPCR, RNA was extracted using the TRIpure Total RNA Extraction Reagent (EP013, ELK Biotechnology, Wuhan, China). According to the manufacturer's protocol, the first-strand cDNA was synthesized using the EntiLink™ 1st Strand cDNA Synthesis Super Mix test kit (EQ031, ELK Biotechnology, Wuhan, China). Real-time PCR was performed and analyzed on a QuantStudio 6 Flex System (Life Technologies, MA, USA) using the EnTurbo™ SYBR Green PCR SuperMix (EQ001, ELK Biotechnology, Wuhan, China). The primers used were:

TGF-β1 forward: 5′-AAGGAGACGGAATACAGGGCT-3′,
TGF-β1 reverse: 5′-ACCTCGACGTTTGGGACTGA-3′,
Samd3 forward: 5′-CCAGCACACAATAACTTGGACC-3′,
Samd3 reverse: 5′-TGAAGCCATCTACTGTCATGGAC-3′,
Actin forward: 5′-CGTTGACATCCGTAAAGACCTC-3′,
Actin reverse: 5′-TAGGAGCCAGGGCAGTAATCT-3′

Table I. Sequences of siRNAs against TGF-β1 and Smad3.

Name		Species		Sequences
R-TGF-β1	NM_021578.2	Rat	NM_021578.2_stealth_638	GAGCAACACGTAGAACTCTACCAGA
			NM_021578.2_stealth_809	CACTGCTCTTGTGACAGCAAAGATA
			NM_021578.2_stealth_1125	CCTACATTTGGAGCCTGGACACACA
			Si RNA_NC	GAGCACAGATGTCAACATCCACAGA
R-Samd3	NM_013095	Rat	NM_013095_stealth_544	CATGAAGAAGGATGAAGTGTGTGTA
			NM_013095_stealth_976	TGGCTTCACTGATCCCTCCAATTCA
			NM_013095_stealth_1277	GGCTTTGAGGCTGTCTACCAGTTGA
			Si RNA_NC	TGGCACTTAGTTCCCAACCTTCTCA

Statistical Analysis

SPSS 25.0 statistical software (IBM Corp., Armonk, NY, USA) was used to analyze the data. The normal distribution of measurement data was expressed as mean ± standard deviation (±SD). No-nnormally distributed data are represented by median and quartile. The *t*-test or Wilcoxon test was used to compare the measurement data between the two groups. The significance level was set at $p < 0.05$.

Results

Roxadustat Rescues Hypoxia-Induced Growth Inhibition

The tubular epithelial cell line (NRE-52E) was selected for our study. Using an *in vitro* hypoxia system, we establish the growth characteristics of these cells with different concentrations of oxygen (1, 5, 10, and 21% O_2) for 24, 48, and 72 hours. All cells grew comparatively within the first 24 hours. At 48 hours, cells in the 1% and 5% O_2 conditions showed significantly lower proliferation rates than the control group (21% O_2) ($p < 0.05$), and by 72 hours, all three hypoxic conditions (1, 5, and 10% O_2) showed significantly delayed proliferation compared to control ($p < 0.05$; Figure 1A).

Previous studies[15] showed that 1% O_2 can induce renal fibrosis in tubular epithelial cells. Hence, we decided to evaluate the effect of different concentrations of roxadustat (0.3, 1, 3, 10, 15 μM) in this hypoxic condition. Roxadustat (RXD) at 1 μM partially restored the growth inhibitory effect of hypoxia at the 72 h time point. With 3 μM RXD, growth recovery was observed at both the 48 and 72 h time points ($p < 0.05$; Figure 1B). Higher concentrations of RXD did not significantly rescue the growth inhibitory effect of hypoxia.

Roxadustat Inhibits Hypoxia-Induced Apoptosis

Culturing NRK-52E cells in hypoxic conditions of 1% or 5% O_2 resulted in a significant increase in apoptosis compared to the control at 72 h ($p < 0.05$; Figure 2). Even though a 10% concentration of O_2 similarly resulted in a decrease in cell proliferation (Figure 1A), there was no considerable increase in apoptosis when compared to the control group ($p > 0.05$; Figure 2). In addition, 3 μM roxadustat significantly decreased apoptosis in both the 1% and 5% O_2 conditions compared to hypoxia treatment alone ($p < 0.05$), indicating that roxadustat inhibits hypoxia-induced apoptosis.

Roxadustat Improves the Morphology of Hypoxic Cells

We observed the differences in cell morphology among the three groups. Most of the NRK-52E cells were round- or oval-shaped in the control group, whereas 1% O_2 hypoxia treatment for 72 h significantly increased many cells' volume. Cells also became sparser, with increased dead cells observed. Cultures with the addition of 3 μM RXD showed healthy cells adhering well on the plate, resembling control cells (Figure 3A). The examination of cellular ultrastructure using electron microscopy revealed that the control cells had intact organelles and maintained membrane integrity. Cells experiencing hypoxia displayed characteristic signs of injury, such as abnormal nuclei, chromatin condensation, nuclear membrane shrinkage, and an increase in apoptotic bodies (shown by red arrows). The administration of roxadustat resulted in enhanced cellular ultrastructure, similar to that observed in the control group (Figure 3B).

Roxadustat Inhibits Hypoxia-Induced HIF-1α Expression

To assess the impact of roxadustat on the expression of HIF-1α, we employed Immunofluorescence as an approach to measure the levels of HIF-1α protein in cells that were cultured at varying oxygen concentrations, both in the presence and absence of roxadustat (Figure 4). All hypoxia conditions significantly increased HIF-1α expression compared to the control at 24, 48 and 72 hours ($p < 0.05$). The addition of 3 μM roxadustat significantly increased HIF-1α expression in the 1% and 5% O_2 conditions but not in the 10% O_2 condition at the 24 h time point ($p < 0.05$). However, by the 48 h time point, RXD treatment no longer increased HIF-1α expression in all hypoxia groups ($p > 0.05$), and after 72 h significantly decreased HIF-1α expression in both the 1% and 5% O_2 hypoxia conditions ($p < 0.05$). Subsequently, the expression levels of TGF-β1 and CTGF were determined through Western blot analysis after 24 h to ascertain any potential changes in their expression resulting from the upregulation of HIF-1α induced by roxadustat. The results showed that there is no increased expression of TGF-β1 and CTGF in the RXD group compared with the hypoxic group ($p > 0.05$;

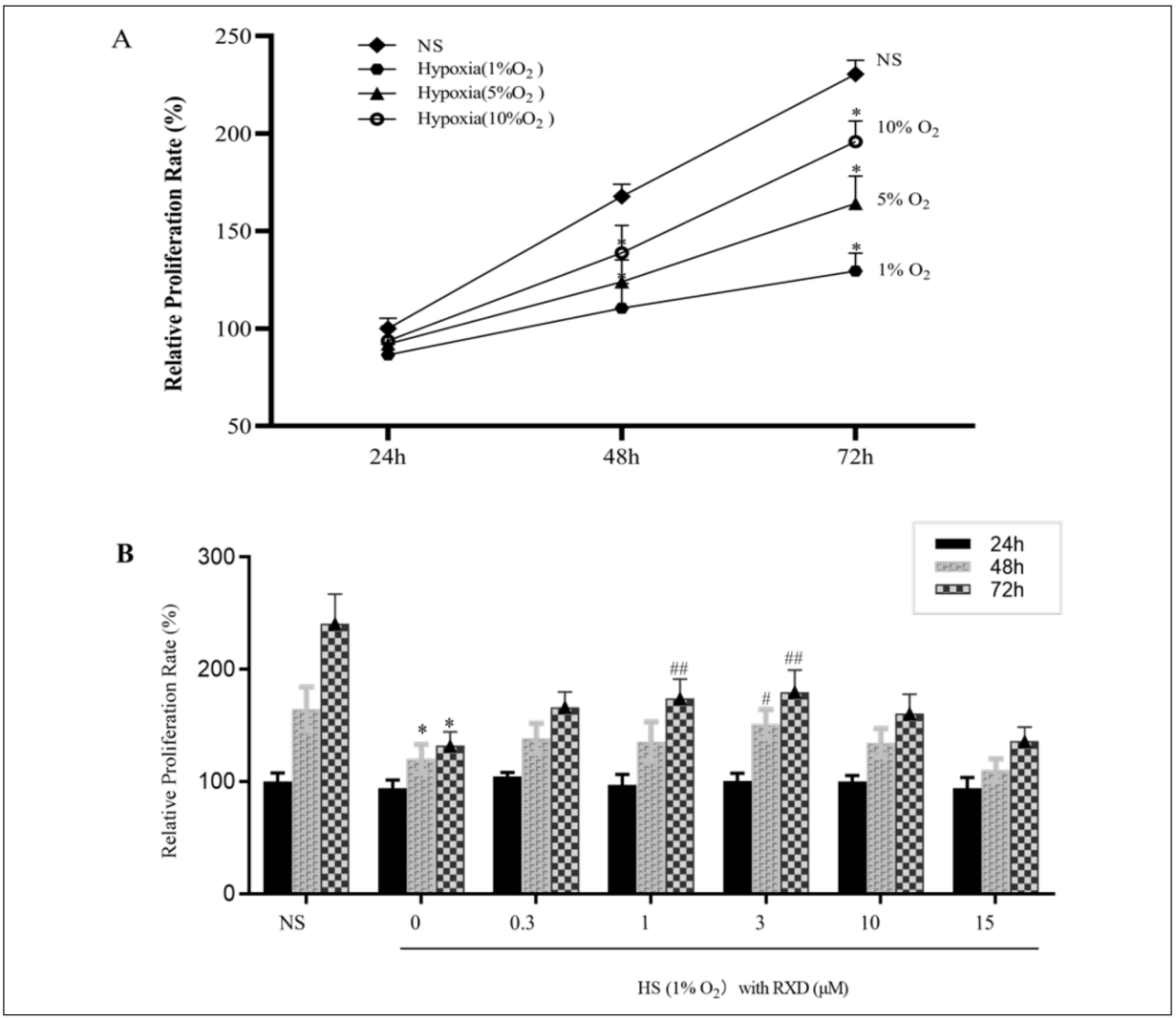

Figure 1. Roxadustat rescues hypoxia-induced growth inhibition. **A**, Proliferation of NRK-52E cells cultured with different oxygen concentrations (1, 5, 10, and 21%) for 24, 48, and 72 hours were detected by CCK-8 analysis. The 21% O_2 condition is the standard cell culture condition and is included as a control (NS). **B**, NRK-52E cells were cultured in normoxia (NS; 21% O_2) or hypoxia (HS; 1% O_2) conditions with different concentrations of roxadustat (RXD: 0, 0.3, 1, 3, 10, and 15 μM) for 24, 48, and 72 hours, followed by cell viability detection with CCK-8 analyses. Data are expressed as mean ± SD; n = 3; $*p < 0.05$ *vs.* NS, $^{\#}p < 0.05$ *vs.* HS + no RXD, $^{\#\#}p < 0.01$ *vs.* HS + no RXD (comparisons were made with the corresponding time points).

Figure 5). Thus, the acute increase in HIF-1α induced by roxadustat does not increase TGF-β1 and CTGF expression.

Roxadustat Inhibits Hypoxia-Induced Protein Expression

Since roxadustat inhibits hypoxia-induced HIF-1α expression at the 72 h time point, we evaluated whether other proteins, including TGF-β1, CTGF, Smad3, p-Smad3, α-SMA, and collagen I, are also affected at this time point. Figure 6 shows that, except for Smad3, all protein levels were increased by 1% O_2 hypoxia compared with the control group ($p < 0.05$). Roxadustat treatment significantly reduced the expression of these proteins to approximately 50% of the level induced by hypoxia ($p < 0.05$), to a level that is more comparable with control cells.

Roxadustat Inhibits TGF-β1/Smad3 Signaling

To determine whether TGF-β1/Smad3 signaling is directly involved in roxadustat regulation of hypoxia-induced changes in the above proteins, we first established TGF-β1 and Smad3 knock-

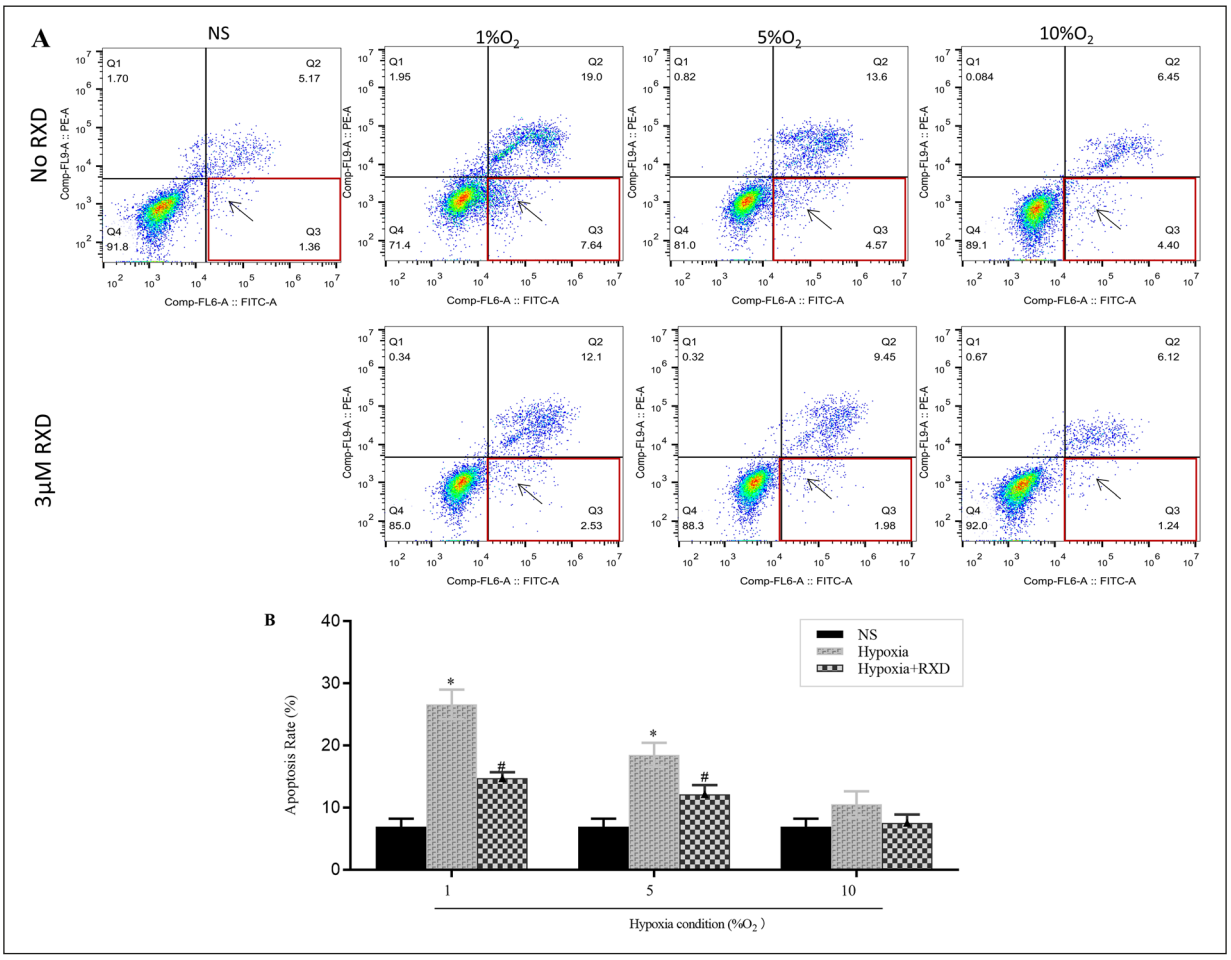

Figure 2. Roxadustat inhibits hypoxia-induced apoptosis. NRK-52E cells were cultured in normoxia (NS; 21% O_2) or hypoxia (HS; 1, 5, and 10% O_2) conditions with 3 μM of roxadustat for 72 h. **A**, Representative flow cytometry plots showing the percentage of apoptotic cells in each condition. **B**, Bar graph summarizing the flow cytometry data. Data presented as mean ± SD; n = 3; *$p < 0.05$ *vs.* NS; $^{\#}p < 0.05$ *vs.* HS.

down cells with siRNAs against these two proteins (Figure 7). Three siRNAs were generated for each protein, and RT-qPCR data showed that the non-template siRNA control did not affect the mRNA expression of either protein. On the other hand, their respective siRNAs significantly decreased mRNA expression of TGF-β1 and Smad3. In both cases, siRNA-1 was more effective in knocking down their respective genes and was chosen for the next experiment.

Following the establishment of the TGF-β1 and Smad3 knockdown cell lines, we evaluated roxadustat's effect after culturing in hypoxia conditions for 72 hours. RXD decreased the protein levels of TGF-β1, p-Smad3, CTGF, and HIF-1α but not Smad3 (Figure 8). siRNA-TGF-β1 treatment also reduced the expression of these proteins compared with the hypoxia group (Figure 8A). Combining siRNA-TGF-β1 with RXD did not further decrease the expression of TGF-β1 and p-Smad3 ($p > 0.05$) but significantly reduced CTGF and HIF-1α ($p < 0.05$). When siRNA-Smad3 was used, all protein expressions were reduced compared with the hypoxia group, except for TGF-β1 (Figure 8B). Combining siRNA-Smad3 with RXD did not further decrease the protein expression of p-Smad3 and HIF-1α compared with the siRNA-Smad3 group ($p > 0.05$) but significantly reduced the expression of TGF-β1 and CTGF ($p < 0.05$). The results of this study suggest that roxadustat exerts a mitigating effect on experimental kidney fibrosis by suppressing the activation of p-Smad3 and TGF-β1. Additionally, roxadustat may modulate the expression of CTGF and HIF-1α *via* other signaling pathways.

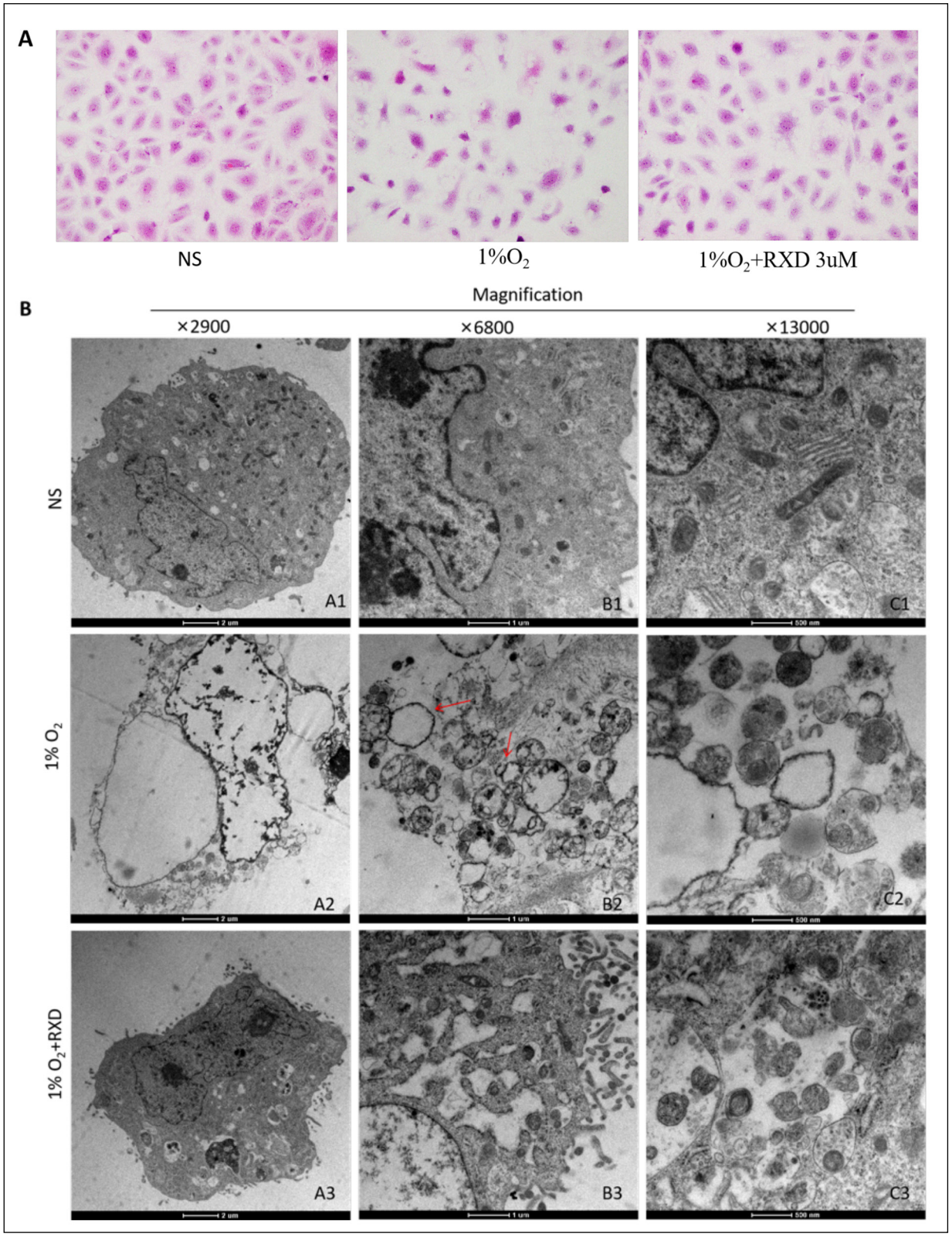

Figure 3. Roxadustat improves the morphology of hypoxic cells. **A**, Representative light microscopy images of eosin-stained NRK-52E cells cultured in standard conditions (NS) or 1% O_2 hypoxia with and without 3 μM RXD for 72 h. Magnification: ×200; (**B**) Representative electron microscopy images of NRK-52E cells cultured in the same conditions as part (**A**). Red arrows: apoptotic bodies.

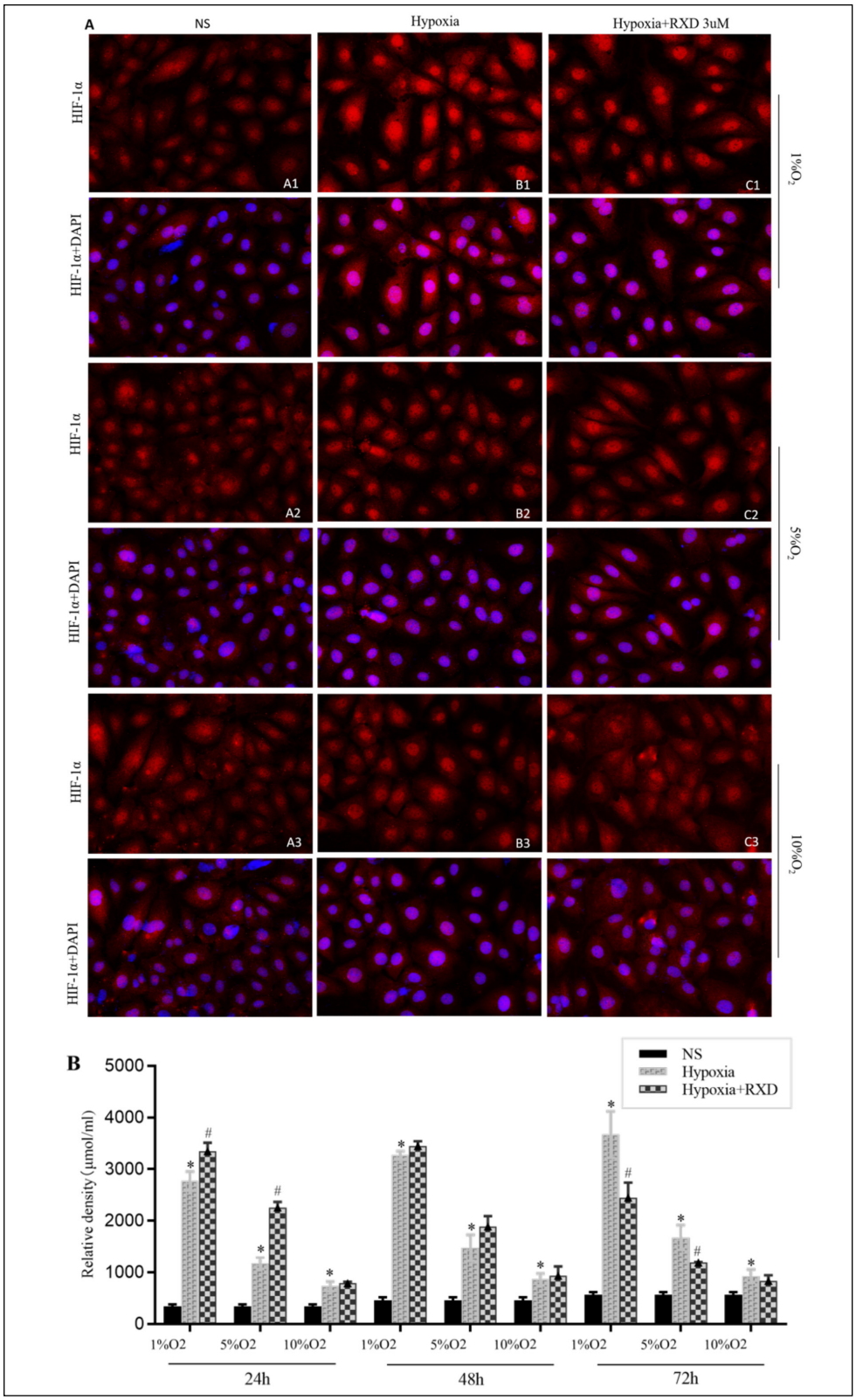

Figure 4. The expression of HIF-1α present "Λ" pattern. **A**, Representative fluorescence images showing HIF-1α staining in NRK-52E cells cultured in normoxia and hypoxia (1, 5, and 10% O_2) conditions with and without 3 μM RXD for 72 h. Magnification ×400. **B**, Bar graph summarizing the staining intensity of HIF-1α in the same culture conditions. Data presented as mean ± SD; n = 3; **p* < 0.05 *vs.* NS, #*p* < 0.05 *vs.* HS. Comparisons were made with the corresponding time points.

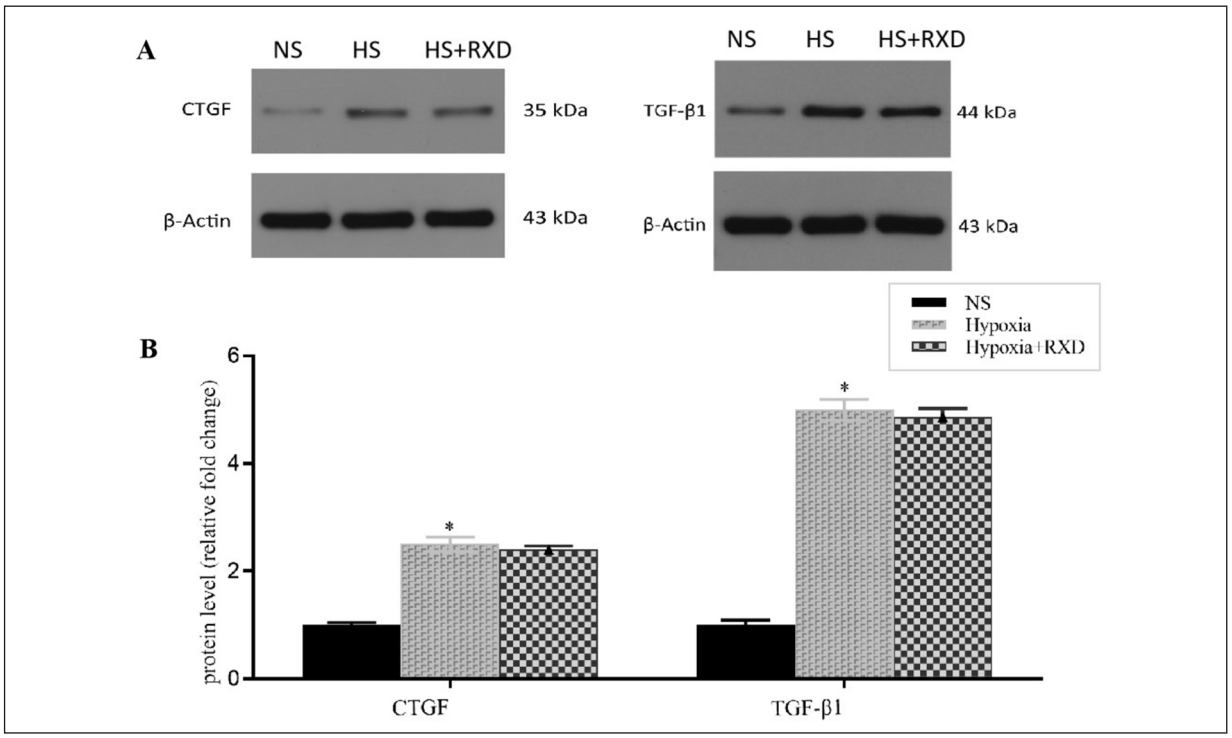

Figure 5. Acute roxadustat-induced HIF-1α expression does not affect TGF-β1 and CTGF expression. **A**, Representative Western blots of NRK-52E cells cultured in normoxia (NS) or hypoxia (1% O_2) conditions with and without 3 μM RXD for 24 h. **B**, Bar graph summarizing the Western blot intensity as an indication of the protein level. Data presented as mean ± SD; n = 3; $^{*}p < 0.05$ *vs.* NS; $^{\#}p < 0.05$ *vs.* HS.

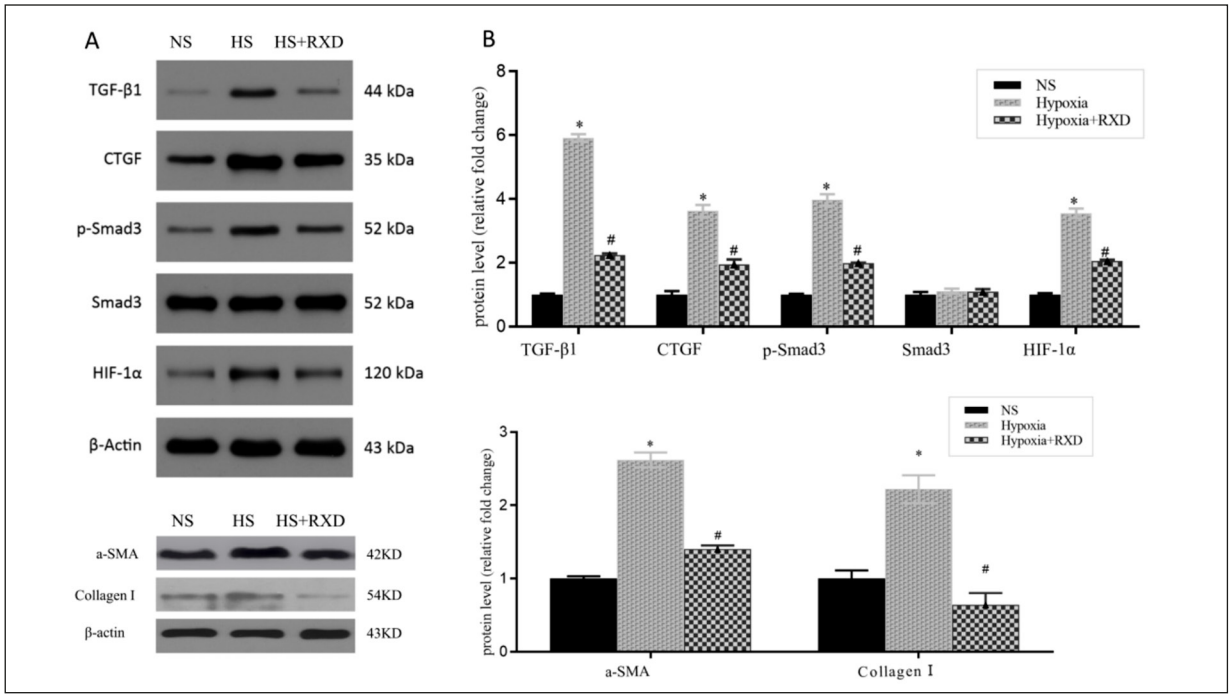

Figure 6. Roxadustat inhibits hypoxia-induced protein expression. **A**, Representative Western blot images of NRK-52E cells cultured in normoxia (NS) or hypoxia (1% O_2) conditions with and without 3 μM RXD for 72 h. **B**, Bar graph summarizing the Western blot intensity as an indication of protein level. Data presented as mean ± SD; n = 3; $^{*}p < 0.05$ *vs.* NS; $^{\#}p < 0.05$ *vs.* HS.

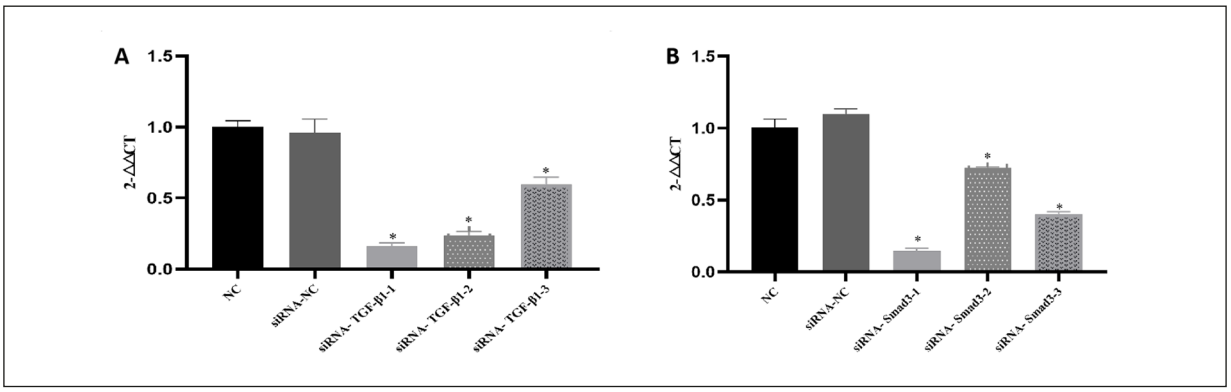

Figure 7. siRNA knockdown of TGF-β1 and Smad3. RT-qPCR bar graphs summarize the relative expression after treatment with their respective siRNAs. **A**, TGF-β1 and (**B**) Smad3. Data presented as mean ± SD; n = 3; **p* < 0.05 *vs*. siRNA-NC.

Discussion

Roxadustat is a hypoxia-inducible factor (HIF) prolyl hydroxylase inhibitor that can enhance HIF transcriptional activity, activate the function of early response target genes encoding proteins such as erythropoietin (EPO) and EPO receptor, promote iron absorption and transport, resulting in coordinated erythropoiesis[1]. Roxadustat has demonstrated favorable safety and efficacy in the treatment of renal anemia.

The function of HIF-1α is not invariable, with effects on renal fibrosis depending on the level of content[2]. Numerous studies[17] have demonstrated that HIF-1α can mitigate cellular damage resulting from ischemia and hypoxia, hence retarding the advancement of renal fibrosis. This is achieved by regulating downstream target genes' expression during the initial phases of chronic kidney disease. However, HIF-1α may aggravate renal fibrosis and promote the development of end-stage renal disease when present in sufficient amounts[18].

Therefore, this study was conducted to observe the changing trend of HIF-1α after roxadustat treatment. Although HIF-1α expression in the roxadustat group was significantly higher at 24 h compared with the hypoxia and control groups, this was reduced at 48 h, with no significant difference between the groups. By 72 h, roxadustat reduced HIF-1α expression compared to the hypoxia group. To determine whether the acute stimulation of HIF-1α by roxadustat is physiologically significant, we examined the protein expression of CTGF and TGF-β1 since CTGF is an HIF target gene and TGF-β1 is recognized as an essential cytokine in the development of renal tubulointerstitial fibrosis. Its overexpression can stimulate mesangial cells, renal tubular epithelial cells, and interstitial cells to synthesize many collagen fibers, fibronectin, and laminin[19]. Our results showed that at 24 h, TGF-β1 and CTGF were significantly increased by hypoxia, but roxadustat treatment did not affect the expression of TGF-β1 and CTGF proteins. This is likely because roxadustat activation of HIF-1α is low and insufficient to increase TGF-β1 and CTGF expression but sufficient to increase erythropoiesis to treat renal anemia.

At 72 h, the expression of TGF-β1, HIF-1α, p-Samd3, CTGF, α-SMA, and collagen I were significantly reduced by roxadustat. Electron microscopy showed that roxadustat can reverse the nuclear envelope shrinkage and increase apoptotic bodies caused by hypoxia. These results suggest a renal-protective effect of roxadustat.

TGF-β1 is a central regulator of cell differentiation, migration, proliferation, and gene expression and can regulate multiple biological processes such as cell proliferation, apoptosis, and autophagy. TGF-β1 can activate myofibroblasts through Smad-dependent or independent pathways, producing an excessive extracellular matrix. Thus, activation of the TGF-β1/Smad3 pathway stimulates fibrosis[20]. We investigated the mechanism of TGF-β1/Smad3 using siRNA. Our study showed that TGF-β1 and p-Smad3 were significantly decreased by siRNA-TGF-β1 with no further additive effect from roxadustat, while CTGF and HIF-1α can be synergistically decreased by combined treatment with siRNA-TGF-β1 and roxadustat. This

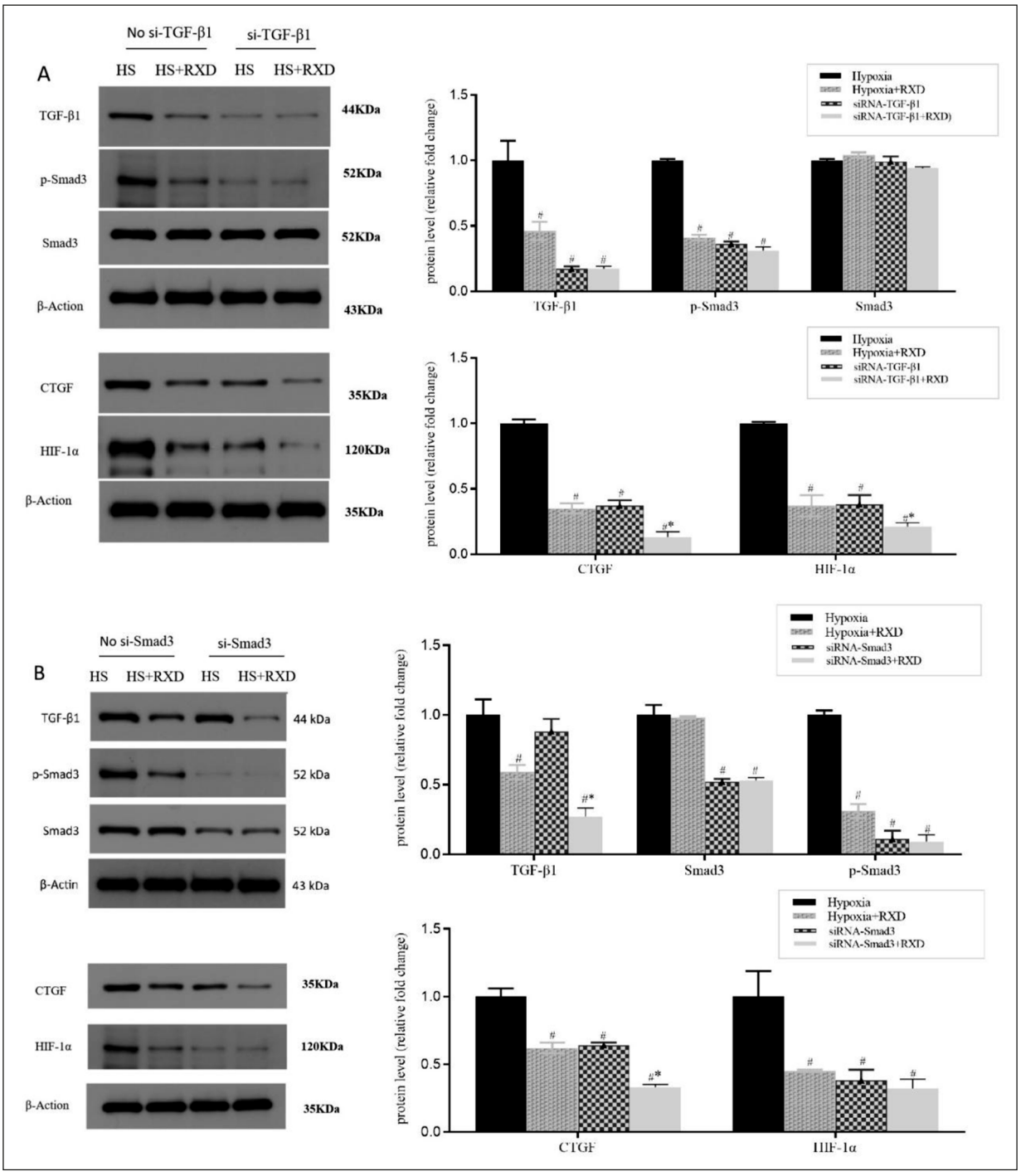

Figure 8. Roxadustat inhibits TGF-β1/Smad3 signaling. NRK-52E cells were cultured in hypoxia (1% O_2) conditions for 72 hours with and without 3 μM RXD, and with and without siRNA to (**A**) TGF-β1 and (**B**) Smad3. Left: representative Western blots; Right: graph summarizing the Western blot's intensity as an indication of protein level. Data presented as mean ± SD; n = 3; *$p < 0.05$ *vs*. siRNA; $^{\#}p < 0.05$ *vs*. HS.

suggests that roxadustat regulates the expression of TGF-β1 and Smad3 directly, while CTGF and HIF-1α are downstream, and roxadustat likely regulates their expression *via* additional pathways. The siRNA-Smad3 treatment also showed CTGF can be synergistically decreased by combined treatment with siRNA-Smad3 and roxadustat.

Limitations

Although this work offers initial observations into the mechanism of renal protection by roxadustat, it is essential to acknowledge certain limitations. We only demonstrated that CTGF and HIF-1α may be regulated *via* additional pathways, not only TGF-β1/Smad3 signaling, which may also be regulated by other HIF-1α related pathways. It should be elucidated with further investigations.

Conclusions

Roxadustat caused a transiently increased expression of HIF-1α, which is insufficient to raise TGF-β1 and CTGF expression. Roxadustat inhibits hypoxia-induced apoptosis *in vitro* and reduces the expression of TGF-β1, CTGF, α-SMA, collagen I, and p-Smad3. Therefore, the renal-protective effect of roxadustat may be mediated, in part, by TGF-β1/Smad3 signaling.

Conflict of Interest

The authors declare that they have no conflict of interests.

Funding

This study was supported by the Sci & Tech Talents of Jiangsu Province (TJ-2021-068), the Development Fund of Affiliated Hospital of Xuzhou Medical University (XYFM202324), Social Development of Science and Technology Projects in Suqian City (No. S201907) and the Suqian Sci & Tech Program (Z202103).

Authors' Contribution

Fangfang Zheng and Mingzuo Zhao experimental designed and were involved in specific experiments and paper writing. Yuanyuan Zhao was involved in specific experiments and writing of the paper. Jinna Wang and Gang Wu experiments carry out data analysis. Longjun Cai experimental design and guidance. Fangfang Zheng and Yuanyuan Zhao contributed equally to this work. All authors read and approved the final version of the manuscript.

Availability of Data and Materials

The data supporting this study's findings are available on request from the corresponding author.

Informed Consent

Not applicable.

Ethics Approval

Not applicable.

ORCID ID

M.-Z. Zhao: 0000-0002-2700-0110
F.-F. Zheng: 0000-0003-4090-8542

References

1) Chen N, Hao C, Peng X, Lin H, Yin A, Hao L, Tao Y, Liang X, Liu Z, Xing C, Chen J, Luo L, Zuo L, Liao Y, Liu BC, Leong R, Wang C, Liu C, Neff T, Szczech L, Yu KP. Roxadustat for Anemia in Patients with Kidney Disease Not Receiving Dialysis. N Engl J Med 2019; 381: 1001-1010.
2) Chen N, Hao C, Liu BC, Lin H, Wang C, Xing C, Liang X, Jiang G, Liu Z, Li X, Zuo L, Luo L, Wang J, Zhao MH, Liu Z, Cai GY, Hao L, Leong R, Wang C, Liu C, Neff T, Szczech L, Yu KP. Roxadustat Treatment for Anemia in Patients Undergoing Long-Term Dialysis. N Engl J Med 2019; 381: 1011-1022.
3) Huang H, Wang X, Zhang X, Wang H, Jiang W. Roxadustat attenuates experimental pulmonary fibrosis in vitro and in vivo. Toxicol Lett 2020; 331: 112-121.
4) Deguchi H, Ikeda M, Ide T, Tadokoro T, Ikeda S, Okabe K, Ishikita A, Saku K, Matsushima S, Tsutsui H. Roxadustat Markedly Reduces Myocardial Ischemia Reperfusion Injury in Mice. Circ J 2020; 84: 1028-1033.
5) Zheng FF, Zhang P, Zhao MZ, Wang JN, Xu XH, Zhang C, Zhang L. Effect of Roxadustat on Factors Associated with Renal Fibrosis and Efficacy. Comput Math Methods Med 2022; 2022: 4764254.
6) Mackensen-Haen S, Bader R, Grund KE, Bohle A. Correlations between renal cortical interstitial fibrosis, atrophy of the proximal tubules and impairment of the glomerular filtration rate. Clin Nephrol 1981; 15: 167-171.
7) Liu BC, Tang TT, Lv LL, Lan HY. Renal tubule injury: a driving force toward chronic kidney disease. Kidney Int 2018; 93: 568-579.
8) Shu S, Wang Y, Zheng M, Liu Z, Cai J, Tang C, Dong Z. Hypoxia and Hypoxia-Inducible Factors in Kidney Injury and Repair. Cells 2019; 8: 207.
9) Ma J, Zhang L, Hao J, Li N, Tang J, Hao L. Up-regulation of microRNA-93 inhibits TGF-β1-induced EMT and renal fibrogenesis by down-regulation of Orai1. J Pharmacol Sci 2018; 136: 218-227.
10) Chen L, Yang T, Lu DW, Zhao H, Feng YL, Chen H, Chen DQ, Vaziri ND, Zhao YY. Central role of dysregulation of TGF-β/Smad in CKD progression and potential targets of its treat-

ment. Biomed Pharmacother 2018; 101: 670-681.

11) Verrecchia F, Rédini F. Transforming Growth Factor-β Signaling Plays a Pivotal Role in the Interplay Between Osteosarcoma Cells and Their Microenvironment. Front Oncol 2018; 8: 133.

12) Mack M, Yanagita M. Origin of myofibroblasts and cellular events triggering fibrosis. Kidney Int 2015; 87: 297-307.

13) Yang PF, Niu YF. Research progress of TGF-β1/Smad signaling pathway in tissue fibrosis. IJPR 2019; 46: 738-744.

14) Muñoz-Sánchez J, Chánez-Cárdenas ME. The use of cobalt chloride as a chemical hypoxia model. J Appl Toxicol 2019; 39: 556-570.

15) Zhang CJ, Li H, Xiong YZ, Chang Y, Yang F, Ma XL, Wang XT, Shimosawa T, Ji ES, Xu QY. Chronic intermittent hypoxia induces renal fibrosis through MR activation. Exp Gerontol 2022; 163: 111780.

16) Zhao LX, Zheng YM, Wang HM, Shi TT. Expression of long non-coding RNA MALAT1 in renal tubular epithelial cells induced by hypoxia and renal fibrosis tissue. Clinical research and practice 2021; 6: 14-18.

17) Yao XB. The role and mechanism of CTSS in renal fibrosis with different degrees of hydronephrosis. Hubei, Wuhan University, 2019.

18) Zhu X, Jiang L, Wei X, Long M, Du Y. Roxadustat: Not just for anemia. Front Pharmacol 2022; 13: 971795.

19) Xing XN, Zhang AP, Guo YS. Research progress of renal fibrosis-related factors. Int J Urol 2011; 31: 271-273.

20) Ying H, Fang M, Hang QQ, Chen Y, Qian X, Chen M. Pirfenidone modulates macrophage polarization and ameliorates radiation-induced lung fibrosis by inhibiting the TGF-β1/Smad3 pathway. J Cell Mol Med 2021; 25: 8662-8675.